Published by Institute of Physics Publishing for SISSA

Received: *June 1, 2005*
Accepted: *June 9, 2005*
Published: *July 4, 2005*

Non-perturbative renormalization of the axial current with dynamical Wilson fermions

Michele Della Morte,[a] Roland Hoffmann,[a] Francesco Knechtli,[a] Rainer Sommer[b] and Ulli Wolff[a]

[a] *Institut für Physik, Humboldt Universität*
Newtonstr. 15, 12489 Berlin, Germany
[b] *DESY*
Platanenallee 6, 15738 Zeuthen, Germany
E-mail: dellamor@physik.hu-berlin.de, roland@physik.hu-berlin.de, knechtli@physik.hu-berlin.de, rainer.sommer@desy.de, uwolff@physik.hu-berlin.de

Abstract: We present a new normalization condition for the axial current, derived from the PCAC relation with non-vanishing quark mass. This condition is expected to reduce mass effects in the chiral extrapolation of the results for the normalization factor Z_{A}. The application to the two-flavor theory with improved Wilson fermions shows that this expectation is indeed fulfilled. Using the Schrödinger functional setup we calculate $Z_{\mathrm{A}}(g_0^2)$ as well as the vector current normalization factor $Z_{\mathrm{V}}(g_0^2)$ for $\beta = 6/g_0^2 \geq 5.2$.

Keywords: Nonperturbative Effects, Lattice QCD.

Contents

1. Introduction

In recent years Wilson's formulation of lattice QCD [1] has matured to a stage where simulations with light dynamical fermions are within reach [2 – 4]. For light quarks some of the most interesting physics at low energies is associated with the pseudo-scalar sector of the theory, whose dynamics is governed by chiral symmetry. It is therefore important to study how and to which extent this symmetry can be realized in our chosen regularization.

For Wilson fermions the (local) isovector axial current is not associated with a symmetry of the lattice action and consequently it does not satisfy continuum Ward-Takahashi identities. However, the latter can be restored up to cutoff-effects (i.e. powers of the lattice spacing) through a finite rescaling of the axial current [5]. Its normalization factor $Z_{\rm A}(g_0^2)$ is exactly obtained in this way by enforcing one particular continuum Ward identity at finite lattice spacing.

Although a perturbative estimate of $Z_{\rm A}$ is available, most of today's simulations are performed at bare gauge couplings $g_0^2 \simeq 1$, where bare perturbation theory cannot be expected to work. To keep systematic effects in physical observables under control, it is therefore mandatory to determine $Z_{\rm A}$ non-perturbatively.

The approach used by the ALPHA Collaboration in the quenched approximation [6] can obviously also be applied to the dynamical case. Here we improve this method by deriving a normalization condition at finite quark mass, which provides a technical advantage

JHEP07(2005)007

when extrapolating the results to the chiral limit. Using the Schrödinger functional setup we compute $Z_{\rm A}(g_0^2)$ for the relevant range of bare gauge couplings. In addition, we check the matching of our non-perturbative estimate with 1-loop perturbation theory through simulations at large β. Systematic effects and in particular $\mathrm{O}(a^2)$ uncertainties arising from a variation of the normalization condition are also considered. These turn out to be rather large for $\beta \lesssim 5.4$.

The paper is organized as follows. After recalling the axial Ward identities we review the normalization condition used in [6] before introducing the new "massive" condition. Numerical results for $Z_{\rm A}$ and $Z_{\rm V}$ are presented in section 3, where we also provide interpolating formulae. In section 4 our conclusions are summarized and we discuss possible applications of the results.

2. Theory

We consider an isospin doublet of quarks with mass m and proceed formally in the continuum theory. The notation employed follows that of [7] and a pedagogical introduction can be found in [8].

2.1 The axial Ward identity in the continuum

By performing local infinitesimal transformations of the quark and anti-quark fields in the euclidean functional integral one derives the Ward identities associated with the flavor chiral symmetry of the action. An axial transformation gives the partially conserved axial current (PCAC) relation

$$\langle \partial_\mu A_\mu^a(x) \mathcal{O} \rangle = 2m \langle P^a(x) \mathcal{O} \rangle \,, \tag{2.1}$$

where

$$A_\mu^a(x) = \overline{\psi}(x)\gamma_\mu\gamma_5 \frac{1}{2}\tau^a \psi(x) \,, \qquad P^a(x) = \overline{\psi}(x)\gamma_5 \frac{1}{2}\tau^a \psi(x) \tag{2.2}$$

are the axial current and the pseudoscalar density, respectively. Here τ^a are the Pauli matrices acting on the flavor indices of the quark fields. The relation (2.1) holds for any operator $\mathcal{O}$ built from the basic fields in a region not containing the point x.

Let $\mathcal{R}$ be a space-time region with smooth boundary $\partial\mathcal{R}$ where the symmetry transformations are applied. The axial current $A_\nu^b(y)$ is inserted as an internal operator ($y \in \mathcal{R}$). If $\mathcal{O}_{\rm ext}$ denotes a polynomial in the basic fields outside this region the integrated form of the axial Ward identity is

$$\int_{\partial\mathcal{R}} \mathrm{d}\sigma_\mu(x) \left\langle A_\mu^a(x) A_\nu^b(y) \mathcal{O}_{\rm ext} \right\rangle - 2m \int_R \mathrm{d}^4x \left\langle P^a(x) A_\nu^b(y) \mathcal{O}_{\rm ext} \right\rangle = i\epsilon^{abd} \left\langle V_\nu^d(y) \mathcal{O}_{\rm ext} \right\rangle . \tag{2.3}$$

The right-hand side of (2.3) originates from the variation of the internal operator $A_\nu^b(y)$ since under chiral transformation the axial current linearly combines with the vector current

$$V_\nu^d(y) = \overline{\psi}(y)\gamma_\nu \frac{1}{2}\tau^d \psi(y) \,. \tag{2.4}$$

In the relation (2.3) we set $\nu = 0$ and choose the region $\mathcal{R}$ to be the space-time volume between the hyper-planes at $y_0 - t$ and $y_0 + t$. After introducing a spatial integration over $\mathbf{y}$ and contracting the isospin indices with the totally antisymmetric tensor ϵ^{abc} we arrive at

$$\begin{aligned}&\int \mathrm{d}^3\mathbf{y} \int_{\partial\mathcal{R}} \mathrm{d}\sigma_\mu(x)\, \epsilon^{abc} \Big\langle A^a_\mu(x) A^b_0(y) \mathcal{O}_{\rm ext} \Big\rangle - \\ &-2m \int \mathrm{d}^3\mathbf{y} \int_{\mathcal{R}} \mathrm{d}^4 x\, \epsilon^{abc} \Big\langle P^a(x) A^b_0(y) \mathcal{O}_{\rm ext} \Big\rangle = 2i \int \mathrm{d}^3\mathbf{y} \Big\langle V^c_0(y) \mathcal{O}_{\rm ext} \Big\rangle . \end{aligned} \tag{2.5}$$

Note that the integral over $\mathcal{R}$ includes a contact term at the point $x = y$. However, power counting and the operator product expansion tell us that the correlation function multiplying the mass has no non-integrable short-distance singularity.

The above equation can be simplified by combining the two contributions from the surface integral over $\partial\mathcal{R}$. We first notice that with periodic boundary conditions in the spatial directions $\int \mathrm{d}^3\mathbf{x}\, \partial_k f(x) = 0$ for any $f(x)$ and thus the integrated form of the PCAC relation (2.1), now written as an operator identity, reads

$$\int \mathrm{d}^3\mathbf{x}\, \partial_0 A^a_0(x) = \int \mathrm{d}^3\mathbf{x}\, \partial_\mu A^a_\mu(x) = 2m \int \mathrm{d}^3\mathbf{x}\, P^a(x) . \tag{2.6}$$

Integrating this relation from $y_0 - t$ to y_0 then results in

$$\int \mathrm{d}^3\mathbf{x}\, A^a_0(y_0 - t, \mathbf{x}) = \int \mathrm{d}^3\mathbf{x}\, A^a_0(y_0, \mathbf{x}) - 2m \int_{y_0 - t}^{y_0} \mathrm{d}x_0 \int \mathrm{d}^3\mathbf{x}\, P^a(x_0, \mathbf{x}) . \tag{2.7}$$

With the region $\mathcal{R}$ defined as above, the integration over the lower surface in (2.5) involves current insertions at $y_0 - t$ and y_0, which can be shifted to y_0 and $y_0 + t$ by using (twice) the partial conservation of the axial current in the form of (2.7). The final result is

$$\begin{aligned}&\int \mathrm{d}^3\mathbf{y}\, \mathrm{d}^3\mathbf{x}\, \epsilon^{abc} \Big\langle A^a_0(y_0 + t, \mathbf{x}) A^b_0(y) \mathcal{O}_{\rm ext} \Big\rangle - \\ &-2m \int \mathrm{d}^3\mathbf{y}\, \mathrm{d}^3\mathbf{x} \int_{y_0}^{y_0 + t} \mathrm{d}x_0\, \epsilon^{abc} \Big\langle P^a(x) A^b_0(y) \mathcal{O}_{\rm ext} \Big\rangle = i \int \mathrm{d}^3\mathbf{y}\, \Big\langle V^c_0(y) \mathcal{O}_{\rm ext} \Big\rangle . \end{aligned} \tag{2.8}$$

Note that this formal manipulation is not invalidated by the contact term in (2.5), which now appears at the lower integration limit.

2.2 Normalization of the axial current on the lattice

A normalization condition for the axial current on the lattice is derived by demanding that eq. (2.8) in terms of the renormalized currents holds at non-zero lattice spacing. While this assumes the knowledge of the renormalization factor of the local vector current, it will become clear that with our choice of $\mathcal{O}_{\rm ext}$ the latter can be easily computed. In the improved theory, eq. (2.8) then defines the normalization factor up to $\mathrm{O}(a^2)$ uncertainties. We construct the relevant matrix elements in the framework of the Schrödinger functional [9, 10]. The notation is taken over from [7], to which we refer for any unexplained symbol.

Our starting point is the improved axial current

$$(A_{\rm I})^a_\mu = A^a_\mu + a c_{\rm A} \tilde{\partial}_\mu P^a , \tag{2.9}$$

where $\tilde{\partial}_\mu$ denotes the symmetric lattice derivative. In a mass-independent renormalization scheme the renormalized (improved) current takes the form [11, 7]

$$(A_{\rm R})^a_\mu = Z_{\rm A}(1 + b_{\rm A} a m_{\rm q})(A_{\rm I})^a_\mu \,. \tag{2.10}$$

Here $m_{\rm q} = m_0 - m_c$ is the bare subtracted quark mass, which on the lattice we need to distinguish from the current quark mass m, derived from a discretized version of (2.1).

In implementing (2.8) on the lattice, we choose the isovector scalar

$$\mathcal{O}^c_{\rm ext} = -\frac{1}{6L^6}\epsilon^{cde}\mathcal{O}'^d\mathcal{O}^e \tag{2.11}$$

as external operator. It is built from the zero momentum sources

$$\mathcal{O}^a = a^6 \sum_{\mathbf{u},\mathbf{v}} \bar{\zeta}(\mathbf{u})\gamma_5 \frac{1}{2}\tau^a \zeta(\mathbf{v}) \tag{2.12}$$

and

$$\mathcal{O}'^a = a^6 \sum_{\mathbf{u},\mathbf{v}} \bar{\zeta}'(\mathbf{u})\gamma_5 \frac{1}{2}\tau^a \zeta'(\mathbf{v})\,, \tag{2.13}$$

where ζ and ζ' are the quark fields at the SF boundary $x_0 = 0$ and $x_0 = T$, respectively. The isospin index of the external operator is contracted with the free index in (2.8). As was shown in [6], isospin symmetry in the form of a vector Ward identity implies that with this setup the right-hand side of eq. (2.8) simplifies to the boundary-to-boundary correlation function

$$f_1 = -\frac{1}{3L^6}\langle \mathcal{O}'^a \mathcal{O}^a \rangle \tag{2.14}$$

up to $\mathrm{O}(a^2)$. This gives the vector current normalization condition, which we will discuss in more detail in the next section.

For the normalization condition derived in [6] ("old" condition) the mass $m_{\rm q}$ was set to zero in (2.8) and (2.10). Since the normalization of the boundary fields cancels as they appear on both sides of (2.8), with the external operator (2.11) the old normalization condition can be written as

$$Z_{\rm A}^2 f^{\rm I}_{\rm AA}(y_0 + t, y_0) = f_1 + \mathrm{O}(a^2)\,, \tag{2.15}$$

with the correlation function

$$f^{\rm I}_{\rm AA}(x_0, y_0) = -\frac{a^6}{6L^6}\sum_{\mathbf{x},\mathbf{y}} \epsilon^{abc}\epsilon^{cde}\left\langle \mathcal{O}'^d (A_{\rm I})^a_0(x)(A_{\rm I})^b_0(y)\mathcal{O}^e \right\rangle . \tag{2.16}$$

In [6] the choice $y_0 = t = T/3$ was made in order to maximize the distance between the current insertions and thus reduce lattice artifacts. Since the mass term in the Ward identity is neglected entirely, an evaluation of this normalization condition at non-vanishing quark mass leads to errors of $\mathrm{O}(r_0 m)$ in addition to the usual $\mathrm{O}(a^2)$ errors. Here we have used r_0, introduced in [12], as a typical low-energy scale.

JHEP07(2005)007

2.3 New normalization condition

We now repeat the above steps using the full axial Ward identity to derive a normalization condition for the axial current. The additional term in eq. (2.8) proportional to the quark mass results in a new correlation function $\tilde{f}_{\mathrm{PA}}^{\mathrm{I}}(y_0+t, y_0)$, which is similar to (2.16) but involves a temporal sum

$$\tilde{f}_{\mathrm{PA}}^{\mathrm{I}}(y_0+t, y_0) = -\frac{a^7}{6L^6} \sum_{x_0=y_0}^{y_0+t} w(x_0) \sum_{\mathbf{x},\mathbf{y}} \epsilon^{abc}\epsilon^{cde} \left\langle \mathcal{O}'^d P^a(x)(A_{\mathrm{I}})_0^b(y)\mathcal{O}^e \right\rangle , \tag{2.17}$$

where

$$w(x_0) = \begin{cases} 1/2, & x_0 = y_0 \;\; \text{or} \;\; y_0+t \\ 1, & \text{otherwise}, \end{cases} \tag{2.18}$$

is introduced in order to implement the trapezoidal rule for discretizing integrals. Due to the aforementioned contact-terms on-shell $\mathrm{O}(a)$ improvement does not apply to the expression (2.17). Therefore, although this new condition removes the $\mathrm{O}(r_0 m)$ uncertainties in the determination of Z_{A} at finite mass, other $\mathrm{O}(am)$ ambiguities appear. In a quenched study [13] this residual mass dependence was shown to be very small.

It follows from the PCAC relation that the product mP^a renormalizes with the same factor as the axial current and hence the new massive normalization condition can be written as

$$Z_{\mathrm{A}}^2(1+b_{\mathrm{A}}am_{\mathrm{q}})^2\Big(f_{\mathrm{AA}}^{\mathrm{I}}(y_0+t,y_0) - 2m\tilde{f}_{\mathrm{PA}}^{\mathrm{I}}(y_0+t,y_0)\Big) = f_1 + \mathrm{O}(am) + \mathrm{O}(a^2) \,. \tag{2.19}$$

In our calculation we neglect the coefficient b_{A}, which is only known perturbatively. This choice only changes the $\mathrm{O}(am)$ effects. The correlation functions for this new normalization condition can be evaluated with the same geometry as for (2.16), i.e. the volume integral covers the middle third of the temporal extension of the lattice.

We now proceed to some technical aspects concerning the evaluation of $f_{\mathrm{AA}}^{\mathrm{I}}$ and $\tilde{f}_{\mathrm{PA}}^{\mathrm{I}}$. Inserting the expression (2.9) for the improved axial current into the correlation functions (2.16) and (2.17) we have

$$\begin{aligned} f_{\mathrm{AA}}^{\mathrm{I}}(x_0,y_0) &= f_{\mathrm{AA}}(x_0,y_0) + ac_{\mathrm{A}}\Big[\tilde{\partial}_0^x f_{\mathrm{PA}}(x_0,y_0) + \tilde{\partial}_0^y f_{\mathrm{AP}}(x_0,y_0)\Big] + \\ &\qquad + a^2 c_{\mathrm{A}}^2\, \tilde{\partial}_0^x\, \tilde{\partial}_0^y\, f_{\mathrm{PP}}(x_0,y_0)\,, \end{aligned} \tag{2.20}$$

$$\tilde{f}_{\mathrm{PA}}^{\mathrm{I}}(y_0+t,y_0) = a \sum_{x_0=y_0}^{y_0+t} w(x_0)\Big[f_{\mathrm{PA}}(x_0,y_0) + ac_{\mathrm{A}}\tilde{\partial}_0^y f_{\mathrm{PP}}(x_0,y_0)\Big]\,, \tag{2.21}$$

$$\text{where: } f_{\mathrm{XY}}(x_0,y_0) = -\frac{a^6}{6L^6}\sum_{\mathbf{x},\mathbf{y}} \epsilon^{abc}\epsilon^{cde}\left\langle \mathcal{O}'^d X^a(x) Y^b(y)\mathcal{O}^e\right\rangle,\;\; X,Y \in \{A_0, P\}\,. \tag{2.22}$$

Performing the Wick contractions for this correlation function, one finds that as a consequence of the isospin structure of the boundary composite fields $\mathcal{O}^a$ and $\mathcal{O}'^a$ only six quark diagrams contribute. Those are shown in figure 1. Among them there are also two disconnected diagrams b) and c), where no propagator connects the $x_0 = 0$ and $x_0 = T$ boundary fields. Exploiting the conservation of the axial current and making use of the

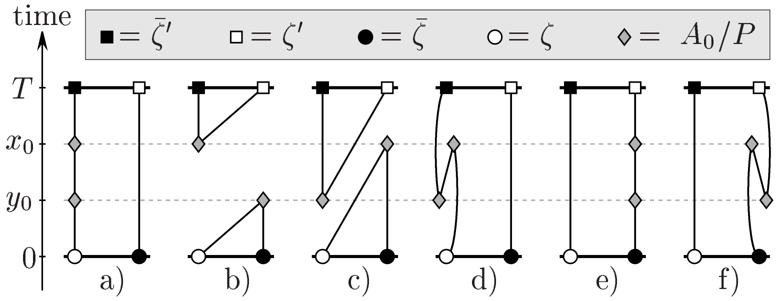

Figure 1: A graphical representation of the possible Wick contractions for the correlation functions $f_{XY}(x_0, y_0)$. The gray diamonds indicate the insertions of Y and X at times y_0 and x_0.

operator product expansion, one can show [14] that in the continuum the diagrams b) and c) cancel for vanishing quark mass (the detailed argument is given in appendix A). This implies that on the lattice they give only an $O(a^2)$ contribution to $f^{\mathrm{I}}_{\mathrm{AA}}$ and $\tilde{f}^{\mathrm{I}}_{\mathrm{PA}}$ in the improved theory. An alternative definition of Z_{A} is thus obtained by using only the connected part of the correlation functions in (2.19).

2.4 The vector current

Isospin symmetry, e.g. in the form of an integrated vector Ward identity, implies that on the lattice

$$Z_{\mathrm{V}}(1 + b_{\mathrm{V}} a m_{\mathrm{q}}) f_{\mathrm{V}}(x_0) = f_1 + \mathrm{O}(a^2)\,, \tag{2.23}$$

where $f_{\mathrm{V}}(x_0)$ is the Schrödinger functional correlation function

$$f_{\mathrm{V}}(x_0) = \frac{a^3}{6L^6} \sum_{\mathbf{x}} i\epsilon^{abc} \langle \mathcal{O}'^a V_0^b(x) \mathcal{O}^c \rangle\,. \tag{2.24}$$

Note that with spatially periodic boundary conditions, the term proportional to the improvement coefficient c_{V} [7, 15] does not contribute to (2.24). In our implementation we also neglect b_{V} and extrapolate the simulation results to zero mass to obtain Z_{V} from (2.23) in the chiral limit. The insertion point x_0 in (2.23) is taken to be $T/2$. The procedure is analogous to the one adopted in the quenched case [6]. There the slope (in am_{q}) of $f_1/(Z_{\mathrm{V}} f_{\mathrm{V}})$ gives an estimate of b_{V}. This is no longer true in the unquenched theory as the improvement coefficient b_{g} is different from zero [7] and thus the slope in am_{q} is not due to b_{V} alone.

3. Numerical results

We performed our simulations using non-perturbatively improved Wilson fermions [7, 16–18] and the plaquette gauge action. The clover coefficient c_{sw} has been set to the value from [17, 18] and for the axial current improvement constant c_{A} we have used the recently determined non-perturbative estimate [19]. Adopting the same setup as in the quenched computation [6, 13] we choose $T = 9/4L$ with periodic boundary conditions in space. The background field is set to zero.

Concerning the algorithm, we employed the HMC with two pseudo-fermion fields as proposed in [20] and studied in the Schrödinger functional in [21] as well as the PHMC algorithm [22, 23]. This choice has been motivated in [24], where PHMC has been shown to be more efficient at the coarsest lattice spacing, since there the spectrum of the improved Wilson-Dirac operator is affected by large cutoff effects in the form of unphysically small eigenvalues.

Summarizing the discussion from section 2.3, we choose the following non-perturbative definitions of the isovector normalization factors

$$Z_{\mathrm{A}}(g_0^2) = \lim_{m\to 0} \sqrt{f_1}\left[f_{\mathrm{AA}}^{\mathrm{I}}\left(\frac{2T}{3},\frac{T}{3}\right) - 2m\tilde{f}_{\mathrm{PA}}^{\mathrm{I}}\left(\frac{2T}{3},\frac{T}{3}\right)\right]^{-1/2}, \tag{3.1}$$

$$Z_{\mathrm{V}}(g_0^2) = \lim_{m\to 0} \frac{f_1}{f_{\mathrm{V}}(T/2)}. \tag{3.2}$$

The quark mass m is defined as in [7] and we average it over three time-slices[1] around $T/2$. The same averaging is used to reduce the statistical error of Z_{V}. Note that in the case of Z_{A} a similar time average would require additional components of the quark propagator. According to the discussion at the end of section 2.3 we define another normalization factor $Z_{\mathrm{A}}^{\mathrm{con}}$ through (3.1), where we now drop the disconnected quark diagrams in the correlation functions.

As discussed in [6], we need to evaluate the normalization conditions on a line of constant physics, keeping all length scales fixed. This ensures that the $\mathrm{O}(a^2)$ ambiguities in the normalization factors vanish smoothly when the perturbative regime is approached. In addition, the normalization conditions have to be set up at zero quark mass since we are aiming for a mass-independent renormalization scheme.

To maintain a line of constant physics we need to know the three values of g_0^2 that yield constant L for $L/a = 8,\ 12,\ 16$. Our value of L is determined by starting with the popular coupling $\beta = 6/g_0^2 = 5.2$ at $L/a = 8$. The readjustments of the bare coupling needed to achieve lattice spacings smaller by factors of 8/12 and 8/16 we take from the 3-loop perturbative formula [25]

$$\frac{a(g_0^2)}{a((g_0')^2)} = e^{-[g_0^{-2}-(g_0')^{-2}]/2b_0}\left[\frac{g_0^2}{(g_0')^2}\right]^{-b_1/2b_0^2}\left[1 + q\,[g_0^2-(g_0')^2] + \mathrm{O}\left((g_0')^4\right)\right], \tag{3.3}$$
$$q = 0.4529(1)\,, \qquad g_0 < g_0'\,.$$

For the range of bare couplings involved this is also consistent with the non-perturbative coupling dependence of r_0/a as checked in [19]. It should in any case be clear to the reader that small deviations from the constant physics line here influence the quality of improvement (size of remaining a^2-effects) but do not imply any systematic errors of the continuum results.

In addition to three matched lattice sizes $L/a = 8,\ 12,\ 16$ at $\beta = 5.2,\ 5.5,\ 5.715$, we simulated at three larger values of β and fixed $L/a = 8$, which corresponds to very small

[1] Four time-slices for odd T.

β	L/a	T/a	κ_c	$Z_{\rm A}$	$Z_{\rm V}$
5.200	8	18	0.135856(18)	0.7141(123)	0.7397(12)
5.500	12	27	0.136733(8)	0.7882(35)(39)	0.7645(22)(18)
5.715	16	36	0.136688(11)	0.8037(38)(7)	0.7801(15)(27)
5.290	8	18	0.136310(22)	0.7532(79)	0.7501(13)
7.200	8	18	0.134220(21)	0.8702(16)(7)	0.8563(5)(45)
8.400	8	18	0.132584(7)	0.8991(25)(7)	0.8838(13)(45)
9.600	8	18	0.131405(3)	0.9132(11)(7)	0.9038(3)(45)

Table 1: Results for the chiral extrapolations of $Z_{\rm A}$ (3.1) and $Z_{\rm V}$ (3.2) and estimates for the critical hopping parameter κ_c.

volumes. This was done in order to verify that our non-perturbative estimate smoothly connects to the perturbative predictions [26 – 28]

$$Z_{\rm A} = 1 - 0.116458\, g_0^2 + {\rm O}(g_0^4)\,, \tag{3.4}$$

$$Z_{\rm V} = 1 - 0.129430\, g_0^2 + {\rm O}(g_0^4)\,. \tag{3.5}$$

Our simulation parameters as well as the final results for $Z_{\rm A}$ and $Z_{\rm V}$ are collected in table 1, where we also include data from simulations at $\beta = 5.29$ and slightly mismatched volume. The latter are only used to qualitatively confirm the observed rapid change of $Z_{\rm A}(g_0^2)$ in this region of the coupling. The results in table 1 are obtained through an interpolation or slight extrapolation in the quark mass. The first error we quote for $Z_{\rm A}$ and $Z_{\rm V}$ is statistical and the second represents our estimate of the systematic error, which originates from deviations from the constant physics condition. It is discussed in the next section. The complete set of simulations results and parameters is given in table 2 in appendix B.

As expected from the above arguments and already verified in the quenched case [13], for the new normalization condition the data exhibit very little dependence on the quark mass. Consequently, uncertainties in the location of the critical point do not propagate to the determination of $Z_{\rm A}$. That this does not hold for the previously used normalization condition [6] can be inferred from figure 2. There we show the chiral extrapolation at $\beta = 5.2$, where we had to use the PHMC algorithm in order to obtain reliable error estimates. With the HMC algorithm the error analysis would have been tainted by the rare occurrence of very small eigenvalues [24]. While for the new normalization condition the slope in am is consistent with zero, the estimate of $Z_{\rm A}$ from the old condition changes by 30% in the (small) mass range shown. We anyway see that for $am \lesssim 0.02$ all mass effects show a linear behavior. For $\beta = 5.5$ the extrapolation is similar to the one shown and at all other gauge couplings we can in fact interpolate from two simulations very close to the critical point.

Our final results are shown in figure 3 as a function of g_0^2. The errors plotted there are obtained by linearly summing the statistical and systematic errors. One can see that our data for both $Z_{\rm A}$ and $Z_{\rm V}$ lie on smooth curves. These can be parameterized by the

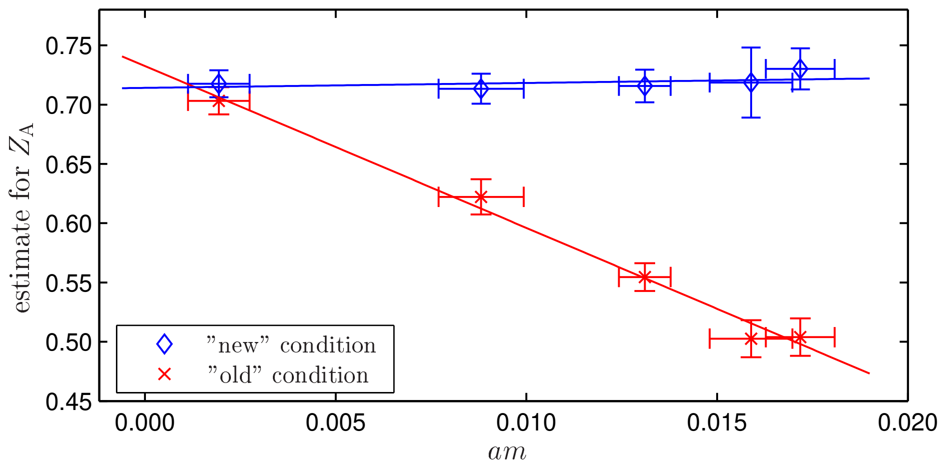

Figure 2: Comparison of the chiral extrapolation at $\beta = 5.2$ using the new and old normalization conditions for $Z_{\rm A}$.

interpolating formulae

$$Z_{\rm A}(g_0^2) = \frac{1 - 0.918\, g_0^2 + 0.062\, g_0^4 + 0.020\, g_0^6}{1 - 0.8015\, g_0^2}\,, \tag{3.6}$$

$$Z_{\rm V}(g_0^2) = \frac{1 - 0.6715\, g_0^2 + 0.0388\, g_0^4}{1 - 0.5421\, g_0^2}\,. \tag{3.7}$$

To $Z_{\rm V}$ we ascribe an absolute error of 0.005, whereas for $Z_{\rm A}$ the absolute error decreases from 0.01 at $\beta = 5.2$ to 0.005 at $\beta = 5.7$. The expressions in (3.6), (3.7) have been obtained by a Pade fit, constrained by 1-loop perturbation theory (3.4), (3.5). Though slightly mismatched and hence excluded from the fit, also the $\beta = 5.29$ data (lighter color in figures 3 and 4) are reproduced by the interpolating formulae in both cases. For $Z_{\rm V}$ we find agreement at the 1% level with the results from [29], where isospin charge conservation is imposed in large volume for matrix elements of the local vector current among nucleon states in the bare coupling range $\beta \leq 5.4$.

We note in passing that similarly to the quenched case [6] also here the use of mean-field improved perturbation theory [30] for $Z_{\rm A/V}$ improves the 1-loop approximation. While the difference to our non-perturbative determination is small for $g_0^2 < 1$, it rapidly increases in the range of physically relevant bare couplings. In particular, at a lattice spacing of roughly 0.1 fm, corresponding to $\beta = 5.2$, our non-perturbative estimate of $Z_{\rm A}$ is almost 20% smaller than the 1-loop value (10% for boosted perturbation theory). In the quenched case [6] this difference was roughly a factor two smaller at the same lattice spacing.[2]

3.1 Systematic effects

Close to the continuum the dependence of the normalization factors on the lattice size is expected to be of order $(a/L)^2$ [6] in the improved theory. This implies that effects in $Z_{\rm A}$ and $Z_{\rm V}$ due to deviations from the line of constant physics should be strongly suppressed.

[2] In fact, in [6] $Z_{\rm A}^{\rm con}$ was considered, but the difference from our definition of $Z_{\rm A}$ was found to be negligible already for $a \simeq 0.1$ fm.

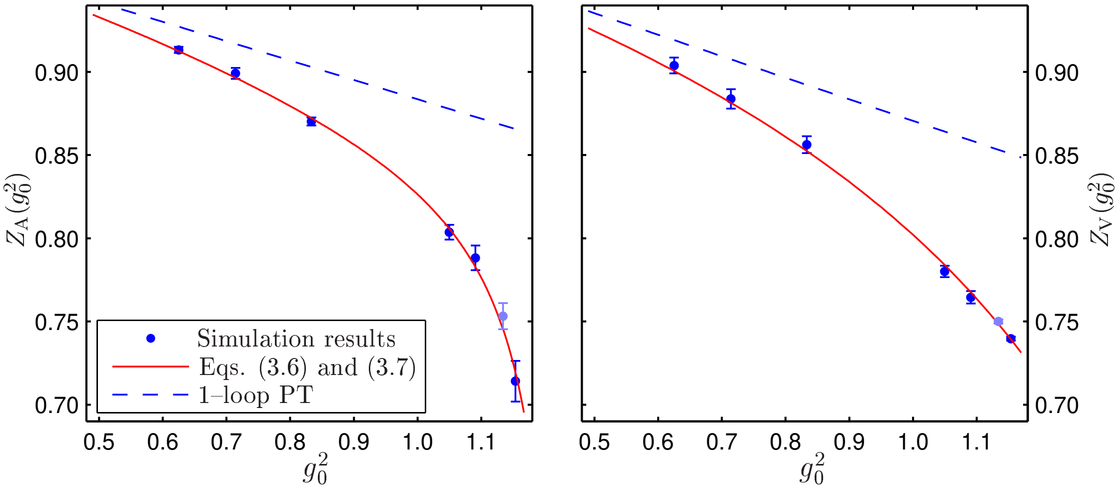

Figure 3: Results for Z_{A} and Z_{V} from numerical simulations and 1-loop perturbation theory (dashed lines). The Pade fits (solid lines) are given by (3.6) and (3.7).

To check for these effects, at $\beta = 5.5$ and 5.715 the simulations closest to the critical point were repeated on smaller lattices ($L/a = 8$ at $\beta = 5.5$ and $L/a = 12$ at $\beta = 5.715$) in order to numerically assess the derivative of $Z_{\mathrm{A/V}}$ with respect to L. Moreover, we estimate the uncertainty in L (measured in units of L at $\beta = 5.2$) due to our approximate matching to increase linearly in β up to at most 10% in the range $5.2 < \beta < 5.715$ (see [19] for a discussion of this estimate). We therefore assign a 6% error to L at $\beta = 5.5$ and 10% at $\beta = 5.715$. Together, this gives the systematic errors quoted in table 1 through a linear propagation of the error. Our results confirm the expected small volume dependence.

For the runs with $\beta \geq 7.2$ the matched L/a would be extremely large. On the other hand the volume dependence should decrease like $g_0^2\,(a/L)^2$ as we are approaching the perturbative regime. In practice the simulations are thus performed at $L/a = 8$ and the systematic error is estimated from additional runs at the coarsest of these lattice spacings, i.e. at $\beta = 7.2$, by taking the difference of Z_{A} and Z_{V} between $L/a = 8$ and 16. While for Z_{A} the volume dependence is hardly visible, in the case of Z_{V} the larger volume ($L/a = 16$) results in a statistically significantly lower value. However, even this amounts only to a 0.5% effect in the final result. In addition, we checked the dependence of Z_{V} on the background field (BF), observing only a moderate effect when going from BF=0 to BF=A (used to define the running coupling $\bar{g}^2$ in [31]) even for $5.2 \leq \beta \leq 5.4$.

3.2 Comparison with an alternative normalization condition

As discussed in section 2.3 the disconnected diagrams in the correlation functions (2.22) are expected to contribute only $\mathrm{O}(a^2)$ to Z_{A}. Hence they can be dropped to obtain an alternative normalization condition for the axial current.

We carry out the previously discussed analysis also with this definition to obtain the results shown in figure 4, where they are compared to the interpolating formula (3.6). The large difference for $g_0^2 \gtrsim 1.1$ has to be interpreted as a cutoff effect and we could

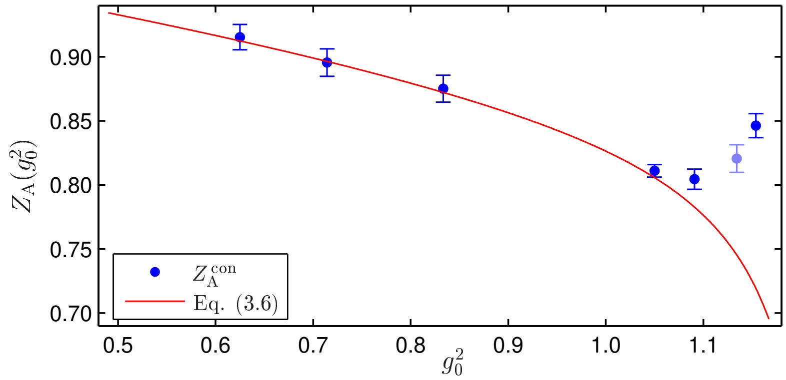

Figure 4: Comparison of $Z_{\rm A}^{\rm con}$ and the interpolating formula (3.6) for $Z_{\rm A}$.

indeed explicitly verify that it vanishes *faster* than linear in a. While this is consistent with the expectations from an improved theory, the magnitude of these lattice artifacts is still worrisome. These findings add further evidence that for $a \simeq 0.1$ fm cutoff effects with dynamical (improved) Wilson fermions can be unexpectedly large [32].

4. Conclusions and outlook

In this work we have shown that in a lattice theory with two flavors of Wilson fermions normalization conditions can be imposed at the non-perturbative level such that isovector chiral symmetries are realized in the continuum limit. Since we are working with an improved theory, chiral Ward-Takahashi identities are then satisfied up to $\mathrm{O}(a^2)$ at finite lattice spacing.

The normalization condition was implemented in terms of correlation functions in the Schrödinger functional framework and evaluated on a line of constant physics in order to achieve a smooth disappearance of the $\mathrm{O}(a^2)$ uncertainties. Through additional simulations at very small lattice spacings and volumes we verified that our non-perturbative definition approaches the perturbative prediction at small bare gauge coupling.

Simulations were done at or near the critical point and owing to the new normalization condition, which keeps track of the mass term in the PCAC relation, any chiral extrapolations are extremely flat. Systematic effects due to deviations from the constant volume condition are also estimated and turn out to be small. The results are well described by an interpolating formula $Z_{\rm A}(g_0^2)$ in the range of bare couplings considered. Enforcing isospin symmetry with the same programme, we obtain at the same time a non-perturbative determination of the normalization constant $Z_{\rm V}(g_0^2)$ of the vector current. Within about 1% it is in agreement with $Z_{\rm V}$ determined in [29] but extends to weak couplings, where contact with perturbation theory is made.

We found rather large $\mathrm{O}(a^2)$ uncertainties in $Z_{\rm A}$ at $\beta < 5.4$ by varying the definition of $Z_{\rm A}$. Together with the algorithmic issues discussed in [24] these findings corroborate the worries expressed in [32] about the status of simulations with improved dynamical Wilson fermions at the currently accessible lattice spacings. This merely emphasizes that cutoff effects in physical quantities can be controlled only if a continuum extrapolation with several lattice resolutions is performed.

The result obtained here is an essential step in the computation of the pseudo-scalar meson decay constant F_{PS} needed to reliably convert the Λ parameter from [31] into physical units. In the short term, together with data from [33] $Z_{\mathrm{A}}(g_0^2)$ will be used in a fully non-perturbative calculation of the strange quark mass following the strategy of [34].

Finally, the method employed here can also be used to obtain Z_{A} in the $\mathrm{O}(a)$-improved three flavor theory with either Iwasaki or plaquette gauge action [18, 35, 36].

Acknowledgments

We are grateful to Martin Lüscher and Stefan Sint for illuminating discussions and Hartmut Wittig for communicating details about the simulations performed for [6]. We thank NIC/DESY Zeuthen for allocating computer time on the APEmille machines for this project. This work is part of the ALPHA collaboration's research programme. It was supported by the Deutsche Forschungsgemeinschaft in the form of the Graduiertenkolleg GK271 and the SFB/TR 09-03. All the computer runs were carried out on machines of the APEmille series at DESY Zeuthen. We thank the staff at DESY Zeuthen for their help.

A. Contribution of disconnected quark diagrams[3]

In figure 1 the diagrams, which are related by an exchange $y_0 \leftrightarrow x_0$ have the same isospin factors with opposite signs. This follows directly from (2.16), where such an exchange corresponds to $\epsilon^{abc} \leftrightarrow \epsilon^{bac}$. Following [14], we now argue that in the massless continuum limit the contributions of the disconnected diagrams b) and c) to $f_{\mathrm{AA}}(x_0, y_0)$ cancel. Considering e.g. diagram b), its continuum version is proportional to

$$f_{\mathrm{AA}}^{\mathrm{b)}}(x_0, y_0) = \int \mathrm{d}^3\mathbf{x}\, \mathrm{d}^3\mathbf{y} \left\langle \mathcal{O}'_{ud}(A_0)_{du}(x)(A_0)_{cs}(y)\mathcal{O}_{sc} \right\rangle, \tag{A.1}$$

where we have introduced flavor indices u, d, s and c for the valence quarks, such that diagram b) is the only possible Wick contraction. Since the spatial insertion points $\mathbf{x}$ and $\mathbf{y}$ are integrated over, $f_{\mathrm{AA}}^{\mathrm{b)}}$ depends on x_0 and y_0 only. In fact, as we are in the chiral limit and the operators $\mathcal{O}$ and $\mathcal{O}'$ generate zero-momentum states, the axial current is conserved and hence the diagram is independent of the insertion points in the two regions $x_0 < y_0$ and $x_0 > y_0$. If the two points meet, contact terms may arise, which we need to treat separately.

To this end we restrict the spatial integration to $|\mathbf{x} - \mathbf{y}| > \epsilon$ and let x_0 approach y_0 from either region. No contact terms can appear due to the finite spatial separation. In the limit $\epsilon \to 0$ the contribution to $f_{\mathrm{AA}}^{\mathrm{b)}}$ from the region $|\mathbf{x}-\mathbf{y}| \leq \epsilon$ vanishes if the integrand has a divergence weaker than $|\mathbf{x} - \mathbf{y}|^{-3}$. In this case we can safely take the limit and conclude that the order of x_0 and y_0 does not play any rôle. This would imply that the diagrams b) and c) have the same value and since their isospin factors have opposite signs, their contributions to f_{AA} cancel.

[3] We thank Martin Lüscher and Stefan Sint for their contributions to a clarification of this issue.

β	κ	L	T	$N_{\rm meas}$	$\tau_{\rm meas}$	am	$Z_{\rm A}$	$Z_{\rm A}^{\rm con}$	$Z_{\rm V}$
5.200	0.13550	8	18	16·200	4	0.01718(90)	0.7301(173)	0.8411(80)	0.7509(6)
5.200	0.13550	8	18	16·40	10	0.0159(11)	0.7186(295)	0.8455(108)	0.7497(14)
5.200	0.13560	8	18	16·225	3	0.01310(68)	0.7157(137)	0.8212(96)	0.7471(7)
5.200	0.13570	8	18	16·230	2	0.0088(11)	0.7134(126)	0.8302(70)	0.7447(8)
5.200	0.13580	8	18	16·230	2	0.00194(81)	0.7176(114)	0.8588(99)	0.7424(14)
5.290	0.13625	8	18	16·50	2	0.0031(18)	0.7527(102)	0.8103(167)	0.7507(19)
5.290	0.13641	8	18	16·120	2	−0.00512(61)	0.7540(124)	0.8378(73)	0.7490(12)
5.500	0.13606	12	27	16·25	6	0.02254(26)	0.8417(222)	0.8077(26)	0.7853(14)
5.500	0.13650	12	27	16·44	3	0.00758(27)	0.7987(153)	0.8100(45)	0.7738(8)
5.500	0.13672	12	27	16·80	3	0.00041(25)	0.7888(32)	0.8048(54)	0.7650(21)
5.500	0.13672	8	18	1·318	4	−0.00168(62)	0.8105(64)	0.8168(38)	0.7750(45)
5.715	0.13665	16	36	1·106	2	0.00194(57)	0.8142(135)	0.8079(31)	0.7827(11)
5.715	0.13670	16	36	1·54	2	−0.00060(69)	0.8004(26)	0.8120(30)	0.7793(20)
5.715	0.13670	12	27	4·62	2	−0.00100(34)	0.8021(38)	0.8182(18)	0.7861(18)
7.200	0.13420	8	18	1·220	2	0.00029(45)	0.8721(24)	0.8772(18)	0.8573(9)
7.200	0.13424	8	18	1·164	2	−0.00028(42)	0.8683(22)	0.8732(18)	0.8553(6)
7.200	0.13424	12	27	16·50	2	−0.00049(15)	0.8685(23)	0.8717(8)	0.8543(18)
7.200	0.13424	16	36	1·80	2	−0.00023(41)	0.8678(18)	0.8670(17)	0.8508(18)
8.400	0.13258	8	18	4·40	2	0.00023(40)	0.8990(28)	0.8956(16)	0.8839(15)
8.400	0.13262	8	18	4·45	2	−0.00183(42)	0.8998(25)	0.8953(13)	0.8826(7)
9.600	0.13140	8	18	4·100	2	0.00021(15)	0.9137(14)	0.9154(7)	0.9040(4)
9.600	0.13142	8	18	4·125	2	−0.00059(15)	0.9118(12)	0.9155(7)	0.9034(4)

Table 2: Summary of simulation parameters and results for $Z_{\rm A}$ and $Z_{\rm V}$.

It is clear that the flavor assignment in (A.1) excludes a single quark bilinear as the leading contribution in the short distance expansion (for $x \to y$) of $A_0(x)A_0(y)$. Hence, by power counting, the latter has (if any) a divergence weaker than $|\mathbf{x}-\mathbf{y}|^{-3}$ in the limit $|\mathbf{x}-\mathbf{y}| \to 0$ and the contribution from the excluded integration region vanishes.

Since the correlation functions approach their continuum value with a rate proportional to a^2, we can conclude that on the lattice the contribution from the disconnected diagrams is a cutoff effect of this order.

B. List of simulation parameters and results

In table 2 the simulation results for $Z_{\rm A}$ and $Z_{\rm V}$ are collected. The number of measurements $N_{\rm meas}$ explicitly contains the number of replica and $\tau_{\rm meas}$ is the number of (unit length) trajectories between consecutive measurements.

References

[1] K.G. Wilson, *Confinement of quarks*, *Phys. Rev.* **D 10** (1974) 2445.

[2] CP-PACS collaboration, A. Ali Khan et al., *Light hadron spectroscopy with two flavors of dynamical quarks on the lattice*, *Phys. Rev.* **D 65** (2002) 054505 [`hep-lat/0105015`].

[3] UKQCD collaboration, C.R. Allton et al., *Effects of non-perturbatively improved dynamical fermions in QCD at fixed lattice spacing*, *Phys. Rev.* **D 65** (2002) 054502 [hep-lat/0107021].

[4] JLQCD collaboration, S. Aoki et al., *Light hadron spectroscopy with two flavors of O(a)-improved dynamical quarks*, *Phys. Rev.* **D 68** (2003) 054502 [hep-lat/0212039].

[5] M. Bochicchio, L. Maiani, G. Martinelli, G.C. Rossi and M. Testa, *Chiral symmetry on the lattice with wilson fermions*, *Nucl. Phys.* **B 262** (1985) 331.

[6] M. Lüscher, S. Sint, R. Sommer and H. Wittig, *Non-perturbative determination of the axial current normalization constant in $O(a)$ improved lattice QCD*, *Nucl. Phys.* **B 491** (1997) 344 [hep-lat/9611015].

[7] M. Lüscher, S. Sint, R. Sommer and P. Weisz, *Chiral symmetry and O(a) improvement in lattice QCD*, *Nucl. Phys.* **B 478** (1996) 365 [hep-lat/9605038].

[8] M. Lüscher, *Advanced lattice QCD*, published in *Proceedings of the Les Houches Summer School, 28 July-5 September 1997*, R. Gupta, A. Morel, E. de Rafael and F. David eds., hep-lat/9802029.

[9] M. Lüscher, R. Narayanan, P. Weisz and U. Wolff, *The Schrödinger functional: a renormalizable probe for nonabelian gauge theories*, *Nucl. Phys.* **B 384** (1992) 168 [hep-lat/9207009].

[10] S. Sint, *On the Schrödinger functional in QCD*, *Nucl. Phys.* **B 421** (1994) 135 [hep-lat/9312079].

[11] K. Jansen et al., *Non-perturbative renormalization of lattice QCD at all scales*, *Phys. Lett.* **B 372** (1996) 275 [hep-lat/9512009].

[12] R. Sommer, *A new way to set the energy scale in lattice gauge theories and its applications to the static force and α_S in* SU(2) *Yang-Mills theory*, *Nucl. Phys.* **B 411** (1994) 839 [hep-lat/9310022].

[13] R. Hoffmann, F. Knechtli, J. Rolf, R. Sommer and U. Wolff, *Non-perturbative renormalization of the axial current with improved Wilson quarks*, *Nucl. Phys.* **129** *(Proc. Suppl.)* (2004) 423 [hep-lat/0309071].

[14] M. Lüscher and S. Sint, private communication, 2003.

[15] S. Sint and P. Weisz, *Further results on O(a) improved lattice QCD to one-loop order of perturbation theory*, *Nucl. Phys.* **B 502** (1997) 251 [hep-lat/9704001].

[16] M. Lüscher, S. Sint, R. Sommer, P. Weisz and U. Wolff, *Non-perturbative O(a) improvement of lattice QCD*, *Nucl. Phys.* **B 491** (1997) 323 [hep-lat/9609035].

[17] ALPHA collaboration, K. Jansen and R. Sommer, *$O(\alpha)$ improvement of lattice QCD with two flavors of Wilson quarks*, *Nucl. Phys.* **B 530** (1998) 185 [hep-lat/9803017].

[18] JLQCD collaboration, N. Yamada et al., *Non-perturbative O(a)-improvement of Wilson quark action in three-flavor QCD with plaquette gauge action*, *Phys. Rev.* **D 71** (2005) 054505 [hep-lat/0406028].

[19] M. Della Morte, R. Hoffmann and R. Sommer, *Non-perturbative improvement of the axial current for dynamical Wilson fermions*, *JHEP* **03** (2005) 029 [hep-lat/0503003].

[20] M. Hasenbusch, *Speeding up the Hybrid-Monte-Carlo algorithm for dynamical fermions*, *Phys. Lett.* **B 519** (2001) 177 [hep-lat/0107019].

[21] ALPHA collaboration, M. Della Morte et al., *Simulating the Schrödinger functional with two pseudo-fermions*, *Comput. Phys. Commun.* **156** (2003) 62 [hep-lat/0307008].

[22] P. de Forcrand and T. Takaishi, *Fast Fermion Monte Carlo*, *Nucl. Phys.* **53** *(Proc. Suppl.)* (1997) 968 [hep-lat/9608093].

[23] R. Frezzotti and K. Jansen, *A polynomial hybrid Monte Carlo algorithm*, *Phys. Lett.* **B 402** (1997) 328 [hep-lat/9702016].

[24] ALPHA collaboration, M. Della Morte, R. Hoffmann, F. Knechtli and U. Wolff, *Impact of large cutoff-effects on algorithms for improved Wilson fermions*, *Comput. Phys. Commun.* **165** (2005) 49 [hep-lat/0405017].

[25] A. Bode and H. Panagopoulos, *The three-loop β-fuction of QCD with the clover action*, *Nucl. Phys.* **B 625** (2002) 198 [hep-lat/0110211].

[26] E. Gabrielli, G. Martinelli, C. Pittori, G. Heatlie and C.T. Sachrajda, *Renormalization of lattice two fermion operators with improved nearest neighbor action*, *Nucl. Phys.* **B 362** (1991) 475.

[27] M. Gockeler et al., *Perturbative renormalisation of bilinear quark and gluon operators*, *Nucl. Phys.* **53** *(Proc. Suppl.)* (1997) 896 [hep-lat/9608033].

[28] S. Sint, private notes, 1996.

[29] QCDSF-UKQCD collaboration, T. Bakeyev et al., *Non-perturbative renormalisation and improvement of the local vector current for quenched and unquenched Wilson fermions*, *Phys. Lett.* **B 580** (2004) 197 [hep-lat/0305014].

[30] G.P. Lepage and P.B. Mackenzie, *On the viability of lattice perturbation theory*, *Phys. Rev.* **D 48** (1993) 2250 [hep-lat/9209022].

[31] ALPHA collaboration, M. Della Morte et al., *Computation of the strong coupling in QCD with two dynamical flavours*, *Nucl. Phys.* **B 713** (2005) 378 [hep-lat/0411025].

[32] ALPHA collaboration, R. Sommer et al., *Large cutoff effects of dynamical Wilson fermions*, *Nucl. Phys.* **129** *(Proc. Suppl.)* (2004) 405 [hep-lat/0309171].

[33] ALPHA collaboration, F. Knechtli et al., *Running quark mass in two flavor QCD*, *Nucl. Phys.* **119** *(Proc. Suppl.)* (2003) 320 [hep-lat/0209025].

[34] ALPHA collaboration, J. Garden, J. Heitger, R. Sommer and H. Wittig, *Precision computation of the strange quark's mass in quenched QCD*, *Nucl. Phys.* **B 571** (2000) 237 [hep-lat/9906013].

[35] CP-PACS collaboration, S. Aoki et al., *Non-perturbative determination of $c_{\rm sw}$ in three-flavor dynamical QCD*, *Nucl. Phys.* **119** *(Proc. Suppl.)* (2003) 433 [hep-lat/0211034].

[36] CP-PACS collaboration, K.I. Ishikawa et al., *Study of finite volume effects in the non-perturbative determination of $c_{\rm sw}$ with the SF method in full three-flavor lattice QCD*, *Nucl. Phys.* **129** *(Proc. Suppl.)* (2004) 444 [hep-lat/0309141].

JHEP07(2005)007